

Title

- COVID-19: Predictive Mathematical Models for the Number of Deaths in South Korea, Italy, Spain, France, UK, Germany, and USA.

Authors

Athanasios S. Fokas,^{1,2,3*} Nikolaos Dikaios,^{2,4} George A. Kastis²

Affiliations

¹ Department of Applied Mathematics and Theoretical physics, University of Cambridge, Cambridge, UK.

² Research Center of Mathematics, Academy of Athens, Athens, Greece.

³ Department of Biomedical Engineering, University of Southern California, Los Angeles, CA, USA.

⁴ Centre for Vision, Speech and Signal Processing, University of Surrey, Guildford, UK.

*Corresponding author. Email: tf227@cam.ac.uk

Abstract

We have recently introduced two novel mathematical models for characterizing the dynamics of the cumulative number of individuals in a given country reported to be infected with COVID-19. Here we show that these models can also be used for determining the time-evolution of the associated number of deaths. In particular, using data up to around the time that the rate of deaths reaches a maximum, these models provide estimates for the time that a plateau will be reached signifying that the epidemic is approaching its end, as well as for the cumulative number of deaths at that time. The plateau is defined to occur when the rate of deaths is 5% of the maximum rate. Results are presented for South Korea, Italy, Spain, France, UK, Germany, and USA. The number of COVID-19 deaths in other counties can be analyzed similarly.

Introduction

COVID-19 is the third coronavirus to appear in the human population in the past two decades; the first was the severe acute respiratory syndrome coronavirus SARS-CoV that caused the 2002 outbreak; the second was the Middle East syndrome coronavirus MERS-CoV responsible for the 2012 outbreak. COVID-19 has now caused a pandemic, which poses the most serious global public health threat since the devastating 1918 H1N1 influenza pandemic that killed approximately 50 million people (in proportion to today's population, this corresponds to 200 million people). The unprecedented mobilization of the scientific community has already led to remarkable progress towards combating this threat, such as understanding significant features of the virus at the molecular level, see for example (1) and (2). In addition, international efforts have intensified towards the development of specific pharmacological interventions; they include, clinical trials using old or relatively new medications and the employment of specific monoclonal antibodies, as well as novel approaches for the production of an effective vaccine. For example, there are ongoing

NOTE: This preprint reports new research that has not been certified by peer review and should not be used to guide clinical practice.

44 clinical trials testing the synthetic protein tocilizumab that binds interleukin-6 (tocilizumab is often
45 used in rheumatoid arthritis), as well as clinical trials involving the infusion to infected patients of
46 plasma from individuals who have recovered from a SARS-CoV-2 infection (3). Also, taking into
47 consideration that the *complement pathway* is an integral component of the innate immune response
48 to viruses, and that complement deposits are abundant in the lung biopsies from SARS-CoV-2
49 patients indicating that this system is presumably overacting (6), it has been suggested that anti-
50 complement therapies may be beneficial to SARS-CoV-2 patients. Further support for this
51 suggestion is provided by earlier studies showing that the activation of various components of the
52 complement system exacerbates the acute respiratory distress syndrome disease associated with
53 SARS-CoV (6). The Federal Drug Administration of USA has granted a conditional approval to
54 the anti-viral medication Remdesivir (7). Unfortunately, the combination of the anti-viral
55 medications lopinavir and ritonavir that are effective against the human immunodeficiency virus
56 has not shown any benefits (4). Similarly, the combination of the anti-malarial medication
57 hydroxychloroquine and the antibiotic azithromycin, is not only ineffective but can be harmful (5).

58 The scientific community is also playing an important role in advising policy makers of possible
59 non-pharmacological approaches to limit the catastrophic impact of the pandemic. For example,
60 following the analysis in (8) of two possible strategies, called mitigation and suppression, for
61 combating the epidemic, UK switched from mitigation to suppression. Within this context, in order
62 to design a long-term strategy, it is necessary to be able to predict important features of the COVID-
63 19 epidemic, such as the final accumulative number of deaths. Clearly, this requires the
64 development of predictive mathematical models.

65 In a recent paper (9) we presented a model for the dynamics of the accumulative number of
66 individuals in a given country that are reported at time t to be infected by COVID-19. This model
67 is based on a particular ordinary differential equation of the Riccati type, which is specified by a
68 *constant parameter* denoting the final total number of infected individuals, and by a *time-dependent*
69 *function*; this function and the above parameter capture the effect of the basic characteristics of the
70 COVID-19 infection as well the effect of the various measures taken by a given country for
71 combating the spread of the infection. Remarkably, although the above Riccati equation is a
72 nonlinear equation depending on time-dependent coefficients, it can be solved in closed form. Its
73 solution depends on the above parameter and function, as well as on a parameter related to the
74 constant arising in integrating this equation.

75
76 In the particular case that the associate time-dependent function is a constant, the explicit solution
77 of the above Riccati equation becomes the classical *logistic formula*. It was shown in (9) that
78 although this formula provides an adequate fit of the given data, is *not* sufficiently accurate for
79 predictive purposes. In order to provide more accurate predictions, we introduced two novel
80 models, called *rational* and *birational*.

81
82 Here we will show that the Riccati equation introduced in (9) can also be used for determining the
83 time evolution of the number, $N(t)$, of deaths in a given country caused by the COVID-19 epidemic.
84 This Riccati equation is specified by the parameter N_f , denoting the final total number of deaths,
85 and by the function $\alpha(t)$; this function together with N_f model the effect of the basic characteristics
86 of the SARS-CoV-2 infection as well as the cumulative effect of the variety of different measures
87 taken by the given country for the prevention and the treatment of this viral infection. In the case
88 that $\alpha(t)$ is a constant, denoted by k , the solution of the above Riccati equation becomes the well-
89 known logistic formula,
90

$$N(t) = \frac{N_f}{1 + \beta e^{-\kappa t}}, \quad (1)$$

where β is the constant of integration. In the case that $\alpha(t)$ is the rational function $kd/l+kt$, the Riccati equation gives the rational formula; this is obtained from the logistic formula by simply replacing the exponential function with the function $(l+dt)^{-k}$, where d and k are constants. The birational formula is similar with the rational formula, but the associated parameters are different before and after a fixed time X ; this constant parameter is either T or in the neighborhood of T , where T denotes the time that the rate of deaths reaches a maximum. The point on the curve depicting N as a function of t corresponding to $t=T$ is known as the *inflection point*.

It turns out that the birational formula, in general, yields better predictions than the rational, which in turn provides better predictions than the logistic. Also, in general, the birational curve is above the curve obtained from the data, whereas the rational curve is below. Thus, the *birational and rational formulas may provide upper and lower bound estimates for the number of deaths at the plateau*. The birational formula can be employed only after the curve approaches its sigmoidal part (a precise criterion of when the birational can be used is discussed in the methods section). For this reason, at the present time the birational formula cannot be used for predictions applicable to the epidemics of Germany and USA.

Fig. 1 depicts the total number of deaths as a function of time after the day that 25 days had occurred, for the epidemics in South Korea, Italy, Spain, France, UK, Germany, and USA.

In this work we implemented the following tasks: (i) We determined the parameters specifying the logistic, rational, and birational formulas using the above data until May 1, 2020. In this way it becomes evident that each of these models *can* fit the data. (ii) We also determined the parameters of the above models using data only a subset of the data. Then, by comparing the predictions of the resulting formulas with the remaining actual data it becomes clear that the rational and birational models generate more accurate predictions. Furthermore, for the cases of Italy and Spain the birational formula is above the data points, suggesting that the birational model may provide an upper bound (as noted earlier, for the epidemics of Germany and USA we fit only the logistic and the rational models). (iii) We computed the time of the plateau as well as the value of N at the plateau using the logistic and the rational models, as well as the birational model in the cases that it is applicable. *The plateau is defined as the point when the rate of deaths is 5% of the maximum rate.*

By implementing the above tasks we find the following estimates for the dates that the plateau will be reached as well as for the number of deaths when this occurs: South Korea plateau on May 18, 2020 with 258 deaths; Italy plateau on June 19, 2020 with 34,399 deaths; Spain plateau on May 25, 2020 with 27,090; France on May 13, 2020 with 26,619 deaths; UK on June 25, 2020 with 38,487 deaths; Germany on June 16, 2020 with 8,702 deaths; USA on June 1, 2020 with 78,532 deaths. The estimates for Italy and Spain may be upper bounds, whereas the remaining estimates are lower bounds.

Results

Table 1 presents the model parameters and the plateau characteristics for the three different models as applied to South Korea, Italy, Spain, France, and UK. For the epidemics of Germany and USA, only the parameters and characteristics of the logistic and rational models are presented; for these countries, the sigmoidal part of their curves had not been reached as of May 1, 2020, and hence the birational formula could not be used for accurate predictions. The calculation of the inflection point

139 requires the time that the derivative of N becomes maximum. For computing this point we used the
140 logistic model (the other models yield similar results). For South Korea, Italy, Spain, France, UK,
141 Germany, and USA, the inflection point occurred at $t=23$, $t=35$, $t=28$, $t=33$, $t=32$, $t=27$, and $t=39$,
142 respectively. This corresponds to March 25, April 4, April 6, April 11, April 15, April 15, and April
143 17, 2020, respectively.

144
145 Fig. 2A presents the actual vs. predicted cumulative number of deaths, due to SARS-CoV-2, as a
146 function of days after 25 deaths were reported, for the epidemic in Korea. A closer view of the
147 fitting curves is presented in Fig. 2B. The logistic, rational, and birational formulas were trained
148 with data up to May 1, 2020, which corresponds to $T+37$. The three models provide accurate fits,
149 as quantified by the coefficient of determination, R^2 , and the Root-Mean-Square Error (RMSE).
150 The logistic model predicts the plateau on May 12, 2020 (71 days after the day that 25 deaths were
151 reported) with a total number of 255 deaths; the rational model predicts a plateau on May 15, 2020
152 (day 74) with 258 deaths; and the birational model predicts a plateau on May 18, 2020 (day 77)
153 with 258 deaths.

154
155 Fig. 3 presents the actual vs. predicted cumulative number of deaths, due to SARS-CoV-2, as a
156 function of days after 25 deaths were reported, for Italy, Spain, France, UK, Germany, and USA.
157 The three models were trained with data up to May 1, 2020, which corresponds to $T+27$, $T+25$,
158 $T+20$, $T+16$, $T+16$, and $T+14$, respectively. For the epidemic of Italy (Fig. 3A), the logistic model
159 predicts a plateau on May 12, 2020 (73 days after the day that 25 deaths were reported) with 27,390
160 deaths; the rational model predicts a plateau on June 9, 2020 (day 101) with 31,976 deaths; and the
161 birational model predicts a plateau on June 19, 2020 (day 111) with 34,399 deaths. Clearly, the
162 logistic model already underestimates the actual plateau day and the number of reported deaths,
163 since on May 1, 2020, (last day of acquired data for this study) the number of deaths for Italy had
164 reached 27,967.

165
166 For the epidemic of Spain (Fig. 3B), the logistic model predicts a plateau on May 7, 2020 (day 59
167 after the day that 25 deaths were reported) with 23,795 deaths; the rational and birational models
168 predicts a plateau on May 25, 2020 (day 77) with 26,581 and 27,090 deaths, respectively. Again,
169 the logistic model already underestimates the actual plateau day and the number of reported deaths,
170 since on May 1, 2020, the number of reported deaths for Spain had reached 24,543.

171
172 For the epidemic of France (Fig. 3C), the logistic model predicts a plateau on May 6, 2020 (58 days
173 after the day that 25 deaths were reported) with 23,828 deaths; the rational model predicts a plateau
174 on May 14, 2020 (day 66) with 25,399 deaths; and the birational model predicts a plateau on May
175 13, 2020 (day 65) with 26,619 deaths. The logistic model underestimates again the actual plateau
176 day and the number of deaths, since on May 1, 2020, there were 24,376 confirmed deaths in France;
177 thus, it is expected that the predicted number of the logistic model will be reached in a few days.

178
179 For the epidemic of the UK (Fig. 3D), the logistic model predicts a plateau on May 15, 2020 (62
180 days after the day that 25 deaths were reported) with 27,433 deaths; the rational model predicts a
181 plateau on June 10, 2020 (day 88) with 33,886 deaths; and the birational model predicts a plateau
182 on June 25, 2020 (day 103) with 38,487 deaths. The logistic model again underestimates the actual
183 plateau day and the number of reported deaths, since on May 1, 2020, there were 26,771 confirmed
184 deaths; it is expected that the predicted number of the logistic model will be reached in a few days.

185
186 For the epidemic of Germany (Fig. 3E), the logistic model predicts a plateau on May 17, 2020 (59
187 days after the day that 25 deaths were reported) with 6,830 deaths; the rational model predicts a
188 plateau on June 16, 2020 (day 89) with 8,702 deaths. For the epidemic of the USA (Fig. 3F), the

189 logistic model predicts a plateau on May 15, 2020 (67 days after the day that 25 deaths were
190 reported) with 64,413 deaths; the rational model predicts a plateau on June 1, 2020 (day 84) with
191 78,532 reported deaths.

192
193 It is evident from the above that whereas each of the three equations (3), (10), and (11) can fit the
194 data quite well, the predictive capacities of these formulas are *quite different*. This is further
195 scrutinized in Fig. 4, where using the epidemic data from Italy, Spain, and France trained with data
196 only until $T+15$, we compared the predictions of the resulting formulas with the actual data at later
197 dates. For the trained data set, $T+15$ corresponds to $t=50$, $t=43$ and $t=48$, for Italy, Spain, and France,
198 respectively. It is clear that each of the 3 models gives a different curve. Furthermore, for Italy (Fig.
199 4A) and Spain (Fig. 4B) the birational model provides an upper bound of the actual $N(t)$, whereas
200 the rational model provides a lower bound which is better estimate than the one obtained via the
201 logistic model. Regarding the birational model, for the cases of Italy and Spain the uppermost
202 curves were obtained by using $X=T$. For France we experimented with different values of X for the
203 birational model. For all such values, the birational curve was always above the rational curve; in
204 order to obtain a curve that is above the actual $N(t)$ for France (so that the resulting formula could
205 perhaps yield an upper bound), it was necessary to choose $X=T-3$. Remarkably, the same result was
206 obtained in (9) when examining an uppermost bound for the number of reported infected
207 individuals.

208 Discussion

209
210 Several useful models elucidating aspect of the COVID-19 pandemic have already appeared in the
211 literature, including (10-19). These references represent only a tiny fraction of more than 3,000
212 publications that have appeared in the last four months in arXiv, medRxiv and bioRxiv.

213 Here, we have modelled the cumulative number N of deaths caused by SARS-CoV-2 in a given
214 country as a function of time, in terms of a Riccati equation. This equation is specified by the
215 constant N_f and the function $\alpha(t)$. Although this Riccati equation is a nonlinear ordinary differential
216 equation containing time dependent coefficients, it can be solved in closed form. For appropriately
217 chosen functions $\alpha(t)$, the solution provides a flexible generalization of the classical logistic formula
218 of equation (1) that has been employed in a great variety of applications, including the modelling
219 of infectious processes.

220 The fact that a is now a function of t has important implications. In particular, it made it possible
221 to construct the rational and birational models. All two models, as well as the logistic model provide
222 good fits for the available data. However, as discussed in detail above, the rational and birational
223 models provide more *accurate predictions*. Furthermore, *the birational model may provide an*
224 *upper bound of the actual $N(t)$, whereas the rational model yields a better lower bound than the*
225 *logistic model.*

226 It is noted that our approach has the capacity for increasing continuously the accuracy of the
227 predictions: as soon as the epidemic in a given country passes the time T , the rational model can be
228 used; furthermore, when the sigmoidal part of the curve is approached, the rational model can be
229 supplemented with the birational model. Also, as more data become available, the parameters of
230 the rational and of the birational models can be re-evaluated; this will yield better predictions.

231
232 By formulating $N(t)$ in terms of a Riccati equation, and by exploring the flexibility of the
233 arbitrariness of $\alpha(t)$, it is possible to decipher basic physiological mechanisms dictating the
234 evolution of $N(t)$. In particular, following the transient stage of the epidemic, it may be envisioned

235 that $\alpha(t)$ becomes a function of N instead of a function of t . This is indeed the case: by plotting α in
236 terms of N is possible to scrutinize a posteriori their relationship; we find that after t approximately
237 equal to $T-7$ the relation between α and $N/25$ becomes, remarkably, *linear*, see Fig. 5.

238
239 As a result of the justifiably draconian measures institutionalized in many countries, the number of
240 the total persons reported infected by COVID-19, in China, South Korea, many European countries,
241 USA, and several other countries, has now passed the inflection point. For the above countries, as
242 shown here, the curve depicting the number of deaths as a function of time is also past the inflection
243 point. Following this expected decline of the “first wave” of infections, it is now contemplated that
244 the lockdown measures will be eased. This appears vital, not only for economical but also for health
245 considerations. Indeed, the psychological impact on the population at large of the current situation
246 is substantial (20); furthermore, it is expected to worsen, especially due to the effect of the post-
247 traumatic disorder. A relatively safe 'exit' strategy avoiding a humanitarian disaster is suggested in
248 (21). In any case, whatever strategy is followed, it is natural to expect that the number of reported
249 infected individuals as well as the number of deaths will begin to grow. At this stage the predictions
250 of the models proposed in (9) and here will not be valid. However, these works will still be valuable:
251 they can be used to compute the additional number of reported infected individuals and deaths
252 caused by easing the lockdown measures. Let us hope that a prudent exit strategy is adopted so that
253 these numbers will not be staggering.

254 **Materials and Methods**

256 We obtained the time-series data for the Coronavirus Disease (COVID-19) for South Korea, Italy,
257 Spain, France, UK, Germany, and USA, from the official site of the European Centre for Disease
258 Prevention and Control (22). We arranged the data in the form of deaths, N , over time measured in
259 days, after the day that the number of deaths reached 25.

260 Throughout this paper, the unknown parameters were determined by employing the *simplex*
261 *algorithm*. This is based on an iterative procedure that does not need information regarding the
262 derivative of the function under consideration. The simplex algorithm is particularly effective for
263 cases where the gradient of the likelihood functions is not easy to calculate. The algorithm creates
264 a ‘random’ simplex of $n + 1$ points, where n is the number of the model parameters that need to be
265 estimated. The constrained variation of the simplex algorithm (23, 24) available in MATLAB[®] was
266 used for all models; an L_1 -norm was employed in the likelihood function to improve robustness
267 (25). Random parameter initializations were used to avoid local minima. The simplex algorithm
268 was chosen because it performed better than the nonlinear least-squares curve fitting algorithms
269 evaluated in this work, namely, the Levenberg-Marquardt (26) and the trust-region-reflective
270 algorithms (27).

271
272 The stability of the fitting procedure was established by using the following simple criterion:
273 different fitting attempts based on the use of a fixed number of data points, must yield curves which
274 have the same form beyond the above fixed points. In this way, it was established that the rational
275 formula could be employed provided that data were available until around the time T , whereas the
276 birational formula could be used only for data available well beyond T .

277
278 The fitting accuracy of each model was evaluated by fitting the associated formula on *all* the
279 available data in a specified set. The relevant parameters specifying the logistic, rational, and
280 birational models are given on table 1.

281 We assume that the function $N(t)$ satisfies the ordinary differential equation

$$\frac{dN}{dt} = a(t) \left(N - \frac{N^2}{N_f} \right). \quad (2)$$

The general solution of this equation is given by (9)

$$N = \frac{N_f}{1 + \beta e^{-\tau}}, \quad \tau = \int \alpha(t) dt, \quad (3)$$

where β is the constant arising from integrating equation (2). In the particular case that $\alpha(t)=k$, equation (3) becomes the logistic formula of equation (1) given in the introduction. If $\alpha(t)$ is given by the rational function below,

$$\alpha(t) = \frac{kd}{1 + kt},$$

then equation (3) becomes the rational formula

$$N = \frac{N_f}{1 + b(1 + dt)^{-k}}. \quad (4)$$

The birational formula is given by

$$N = \begin{cases} \frac{c}{1+b(1+dt)^{-k}}, & t \leq X \\ \frac{c}{1+b(1+dX)^{-k}} + \frac{c_1}{1+b_1(1+d_1X)^{-k_1}} - \frac{c_1}{1+b_1(1+d_1t)^{-k_1}}, & t > X \end{cases} \quad (5)$$

Where the fixed parameter X is either T or in the neighborhood of T . For the birational model

$$a(t) = \begin{cases} \frac{kd}{1+dt}, & t \leq X \\ \frac{k_1 d_1}{1+d_1 t} \frac{1}{1 + \left(1 - \frac{c_1}{N_f}\right) (1+d_1 t)^{-k_1}}, & t > X \end{cases} \quad (6)$$

Letting in equation (5) $t \rightarrow \infty$ we find:

$$N_f = \frac{c}{1 + b(1 + dX)^{-k}} - \frac{c_1}{1 + b_1(1 + d_1X)^{-k_1}} + c_1. \quad (7)$$

If b, c, d, k , are close to b_1, c_1, d_1, k_1 , then N_f is close to c_1 , and hence the value of $a(t)$ after $t=X$ is close to the value of $a(t)$ before $t=X$.

The constant T can be computed by solving the equation obtained by equating to zero the second derivative of N . This implies that for the logistic and the rational models T is given respectively by

$$T = \frac{\ln(\beta)}{k}, \quad (1 + dT)^k = b \left(\frac{k-1}{k+1} \right). \quad (8)$$

312 Similarly, for the birational model where the parameters b , d , k , in the second equations (8) are
313 replaced with b_l , d_l , k_l , respectively.

314 References and Notes

- 316 1. P. Zhou, X.-L. Yang, X.-G. Wang, B. Hu, L. Zhang, W. Zhang, H.-R. Si, Y. Zhu., B. Li,
317 C.-L. Huang, H. D. Chen, J. Chen, Y. Luo, H. Guo, R. D. Jiang, M. Q. Liu, Y. Chen, X. R.
318 Shen, X. Wang, X. S. Zheng, K. Zhao, Q. J. Chen, F. Deng, L. L. Liu, B. Yan, F. X. Zhan,
319 Y. Y. Wang, G. F. Xiao GF, Z. L. Shi., A pneumonia outbreak associated with a new
320 coronavirus of probable bat origin. *Nature*, **579**, 270–273 (2020).
- 321 2. J. Shang, G. Ye, K. Shi, Y. Wan, C. Luo, H. Aihara, Q. Geng, A. Auerbach, F. Li, Structural
322 basis of receptor recognition by SARS-CoV-2. *Nature* (2020) (*in press*).
- 323 3. A. Bhimraj, R. L. Morgan, A. H. Shumaker, V. Lavergne, L. Baden, V. C. Cheng, K. M.
324 Edwards, R. Gandhi, W. J. Muller, J. C. O’Horo, S. Shoham, M. H. Murad, R. A. Mustafa,
325 S. Sultan, Y. Falck-Ytter. Infectious Diseases Society of America Guidelines on the
326 Treatment and Management of Patients with COVID-19 Infection, IDSA (2020).
- 327 4. B. Cao, Y. Wang, D. Wen, W. Liu, J. Wang, G. Fan, L. Ruan, B. Song, Y. Cai, M. Wei, X.
328 Li, J. Xia J, N. Chen, J. Xiang, T. Yu, T. Bai, X. Xie, L. Zhang, C. Li, Y. Yuan, H. Chen,
329 H. Li, H. Huang, S. Tu, F. Gong, Y. Liu, Y. Wei, C. Dong, F. Zhou, X. Gu, J. Xu, Z. Liu,
330 Y. Zhang, H. Li, L. Shang, K. Wang, K. Li, X. Zhou, X. Dong, Z. Qu, S. Lu, X. Hu, S.
331 Ruan, S. Luo, J. Wu, L. Peng, F. Cheng, L. Pan, J. Zou, C. Jia, J. Wang, X. Liu, S. Wang,
332 X. Wu, Q. Ge, J. He, H. Zhan, F. Qiu, L. Guo, C. Huang, T. Jaki, F. G. Hayden, P. W.
333 Horby, D. Zhang, C. Wang. A trial of lopinavir–ritonavir in adults hospitalized with severe
334 Covid-19. *New England Journal of Medicine*, **382**, 1787-1799 (2020).
- 335 5. J. Magagnoli, S. Narendran, F. Pereira, T. Cummings, J. W. Hardin, S. Scott Sutton, J.
336 Ambati, Outcomes of hydroxychloroquine usage in United States veterans hospitalized with
337 Covid-19, *medRxiv* (2020).
- 338 6. A. M. Risitano, D. C. Mastellos, M. Huber-Lang, D. Yancopoulou, C. Garlanda, F. Ciceri,
339 J. D. Lambris, Complement as a target in COVID-19?. *Nat. Rev. Immunol* (2020).
- 340 7. [https://www.fda.gov/news-events/press-announcements/coronavirus-covid-19-update-fda-
341 issues-emergency-use-authorization-potential-covid-19-treatment](https://www.fda.gov/news-events/press-announcements/coronavirus-covid-19-update-fda-issues-emergency-use-authorization-potential-covid-19-treatment).
- 342 8. N. M. Ferguson, D. Laydon, G. Nedjati-Gilani, N. Imai, K. Ainslie, M. Baguelin, S. Bhatia,
343 A. Boonyasiri, Z. Cucunubá, G. Cuomo-Dannenburg, A. Dighe, I. Dorigatti, H. Fu, K.
344 Gaythorpe, W Green, A. Hamlet, W. Hinsley, L. C. Okell, S. van Elsland, H. Thompson, R.
345 Verity, E. Volz, H. Wang, Y. Wang, P. G. T. Walker, C. Walters, P. Winskill, C. Whittaker,
346 C. A. Donnelly, S. Riley, A. C. Ghani. Impact of nonpharmaceutical interventions (NPIs)
347 to reduce COVID-19 mortality and healthcare demand. London: Imperial College COVID-
348 19 Response Team, *Report 9*. (2020).
- 349 9. A. S. Fokas, N. Dikaïos, G. A. Kastis, Predictive mathematical models for the number of
350 individuals infected with COVID-19. *medRxiv* (2020).
- 351 10. S. B. Bastos, D. O. Caljueiro. Modeling and forecasting the early evolution of the Covid-19
352 pandemic in Brazil. *arXiv:2003.14288* (2020).
- 353 11. C. Qi, D. Karlsson, K. Sallmen, R. Wyss, Model studies on the COVID-19 pandemic in
354 Sweden. *arXiv:2004.01575* (2020).
- 355 12. E. Gjini, Modeling Covid-19 dynamics for real-time estimates and projections: an
356 application to Albanian data. *medRxiv* 2020.03.20.20038141 (2020).
- 357 13. E. Kaxiras, G. Neofotistos, E. Angelaki. The first 100 days: modeling the evolution of the
358 COVID-19 pandemic, *arXiv:2004.14664* (2020).
- 359 14. C. Yang, J. Wang, A mathematical model for the novel coronavirus epidemic in Wuhan,
360 China, *Math. Biosci. Eng.* **17**, 2708-2724 (2020).

- 361 15. K.-M. Tam, N. Walker, J. Moreno. Projected Development of COVID-19 in Louisiana.
362 *arXiv:2004.02859* (2020).
- 363 16. A. Arenas, W. Cota, J. Gomez-Gardenes, S. Gómez, C. Granell, J. T. Matamalas, D.
364 Soriano-Panos, B. Steinegger, A mathematical model for the spatiotemporal epidemic
365 spreading of COVID19. *medRxiv* 2020.03.21.20040022 (2020).
- 366 17. L. Danon, E. Brooks-Pollock, M. Bailey, M. Keeling, A spatial model of CoVID-19
367 transmission in England and Wales: early spread and peak timing, *medRxiv*
368 2020.02.12.20022566 (2020).
- 369 18. L. Russo, C. Anastassopoulou, A. Tsakris, G.N. Bifulco, E.F. Campana, G. Toraldo, C.
370 Siettos. Tracing DAY-ZERO and Forecasting the Fade out of the COVID-19 Outbreak in
371 Lombardy, Italy: A Compartmental Modelling and Numerical Optimization Approach.
372 *medRxiv* 2020.03.17.20037689 (2020).
- 373 19. C. Anastassopoulou, L. Russo, A. Tsakris, C. Siettos. Data-based analysis, modelling and
374 forecasting of the COVID-19 outbreak. *PLOS ONE* **15**, e0230405 (2020).
- 375 20. S. K. Brooks, R. K. Webster, L. E. Smith, L. Woodland, S. Wessely, N. Greenberg, G. J.
376 Rubin, The psychological impact of quarantine and how to reduce it: rapid review of the
377 evidence, *The Lancet*, **395**, 912 – 920 (2020).
- 378 21. A. S. Fokas, J. Cuevas-Maraver, P. G. Kevrekidis, Two alternative scenarios for easing
379 COVID-19 lockdown measures: one reasonable and one catastrophic (preprint)
- 380 22. <https://www.ecdc.europa.eu/en/geographical-distribution-2019-ncov-cases>
- 381 23. J. D. Errico, Bound Constrained Optimization, Computer Program. MATLAB and Simulink
382 Centre, *The MathWorks, Inc.* (2005).
- 383 24. J. C. Lagarias, J. A. Reeds, M. H. Wright, P. E. Wright, Convergence Properties of the
384 Nelder-Mead Simplex Method in Low Dimensions. *SIAM Journal on Optimization* **9**, 112–
385 147 (1998).
- 386 25. W. H. Press, S. A. Teukolsky, W. T. Vetterling, B. P. Flannery, Numerical Recipes in C.
387 Cambridge university press, Cambridge, New York. (1994).
- 388 26. J. J. Moré, The Levenberg-Marquardt Algorithm: Implementation and Theory. Numerical
389 Analysis, ed. G. A. Watson, *Lecture Notes in Mathematics* **630**, Springer Verlag, 105–116.
390 (1977).
- 391 27. T. F. Coleman, Y. Li, An Interior, Trust Region Approach for Nonlinear Minimization
392 Subject to Bounds. *SIAM Journal on Optimization*, **6**, 418–445 (1996).

393 Acknowledgments

395 **General:** A.S.F is grateful to several colleagues and in particular to the neurologist M.
396 Dalakas and the mathematician S. Kourouklis for encouraging him to be involved with the
397 modelling of COVID-19.

398
399 **Funding:** A.S.F. acknowledges support from EPSRC, UK, in the form of a Senior
400 Fellowship. N.D. acknowledges support from Royal Society in the form of a fellowship.
401

402 **Author contributions:** A.S.F. conceived, designed and supervised the study. N.D. and
403 G.A.K. performed the fitting experiments and analysis of the results. A.S.F. wrote the initial
404 draft of the manuscript. All authors critically revised and improved the manuscript in
405 various ways. All authors reviewed the manuscript and gave final approval for publication.
406

407 **Competing interests:** The authors declare no competing interests.

408 **Data and materials availability:** All data needed to evaluate the conclusions in the paper
409 are present in the paper and/or the Supplementary Materials.

Figures and Tables

Table 1. Model parameters and plateau characteristics. The model parameters and the plateau characteristics for the three different models are presented for South Korea, Italy, Spain, France, and UK. For the epidemics of Germany and USA only the parameters and characteristics of the logistic and rational models are presented. For those countries, the sigmoidal part of the curves had not been reached as of May 1, 2020 and hence the birational formula could not be used for accurate predictions.

		South Korea	Italy	Spain	France	UK	Germany	USA
Logistic model	N_f	259	27,687	24,016	24,124	27,708	6,906	65,027
	k	0.0871	0.1188	0.1481	0.1743	0.1533	0.1430	0.1645
	b	7.6672	63.4044	65.7474	305.1352	134.8143	51.2444	583.1774
	T	23	35	28	33	32	27	39
	Plateau (days)	71	73	59	58	62	59	67
	Plateau (deaths)	255	27,390	23,765	23,828	27,433	6,830	64,413
	R^2	0.9988	0.9955	0.9955	0.9977	0.9975	0.9979	0.9984
	$RMSE$	3	678	607	445	475	102	867
Rational model	N_f	263	33,153	27,524	26,035	34,920	9021	80260
	k	27.2451	3.6299	3.8035	7.3695	4.0954	3.7379	6.6719
	b	8.5207	4,892.02	6,372.6	2,894.71	23,496.07	451.2287	19,330.79
	d	.0034	0.2455	0.2996	0.0586	0.2997	0.12828	0.08069
	Plateau (days)	74	101	77	66	88	89	84
	Plateau (deaths)	258	31,976	26,581	25,399	33,886	8,702	78,532
	R^2	0.9988	0.9994	0.9994	0.9991	0.9996	0.9994	0.9993
	$RMSE$	3	262	233	280	199	55	570
Birational model	k	3.6330	6.7118	5.0583	9.4433	4.4465		
	b	8.38	953.44	6,532.56	1,958.95	39,666.12		
	c	243	23,310	21,434	31,065	29,724		
	d	0.0342	0.0572	0.1814	0.0354	0.3000		
	k_l	5.4485	4.0093	4.6349	12.3054	3.5263		
	b_l	12.57	478.17	9,787.64	2,441.23	27,864.22		
	c_l	322	31,737	21,766	18,873	38,492		
	d_l	0.0283	0.0893	0.1796	0.0235	0.4354		
	Plateau (days)	77	111	77	65	103		
	Plateau (deaths)	258	34,399	27,090	26,619	38,487		
	R^2	0.9988	1.0000	0.9999	0.9994	0.9998		
$RMSE$	3	60	82	235	148			

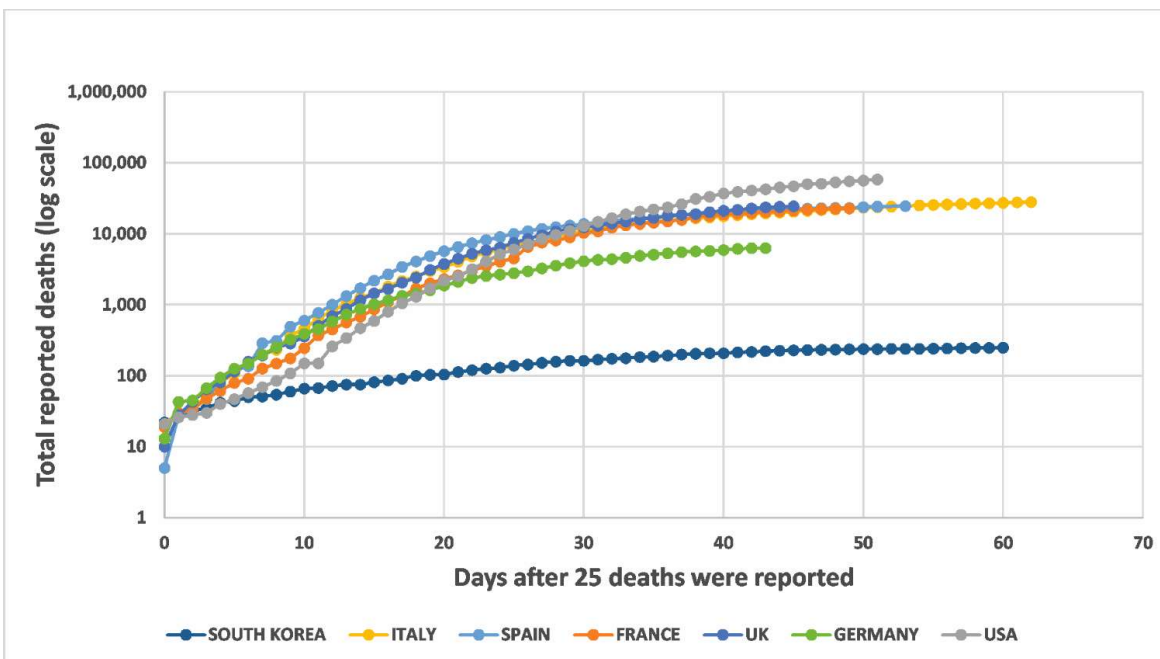


Fig. 1. Total deaths vs days after 25 deaths were reported. COVID-19 virus epidemics in South Korea, Italy, Spain, France, United Kingdom, Germany and United States of America: Total cumulative number of deaths due to SARS-CoV-2 reported up to May 1, 2020, as a function of days after the day that 25 deaths were reported.

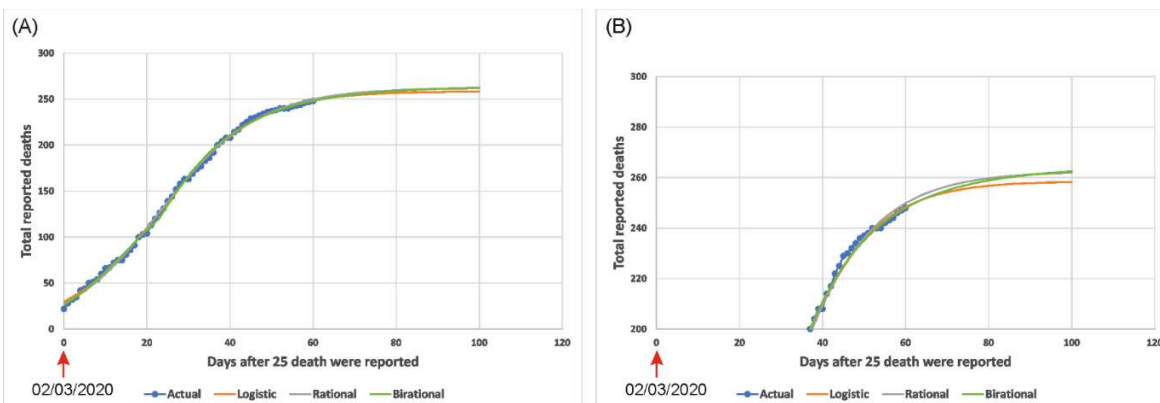
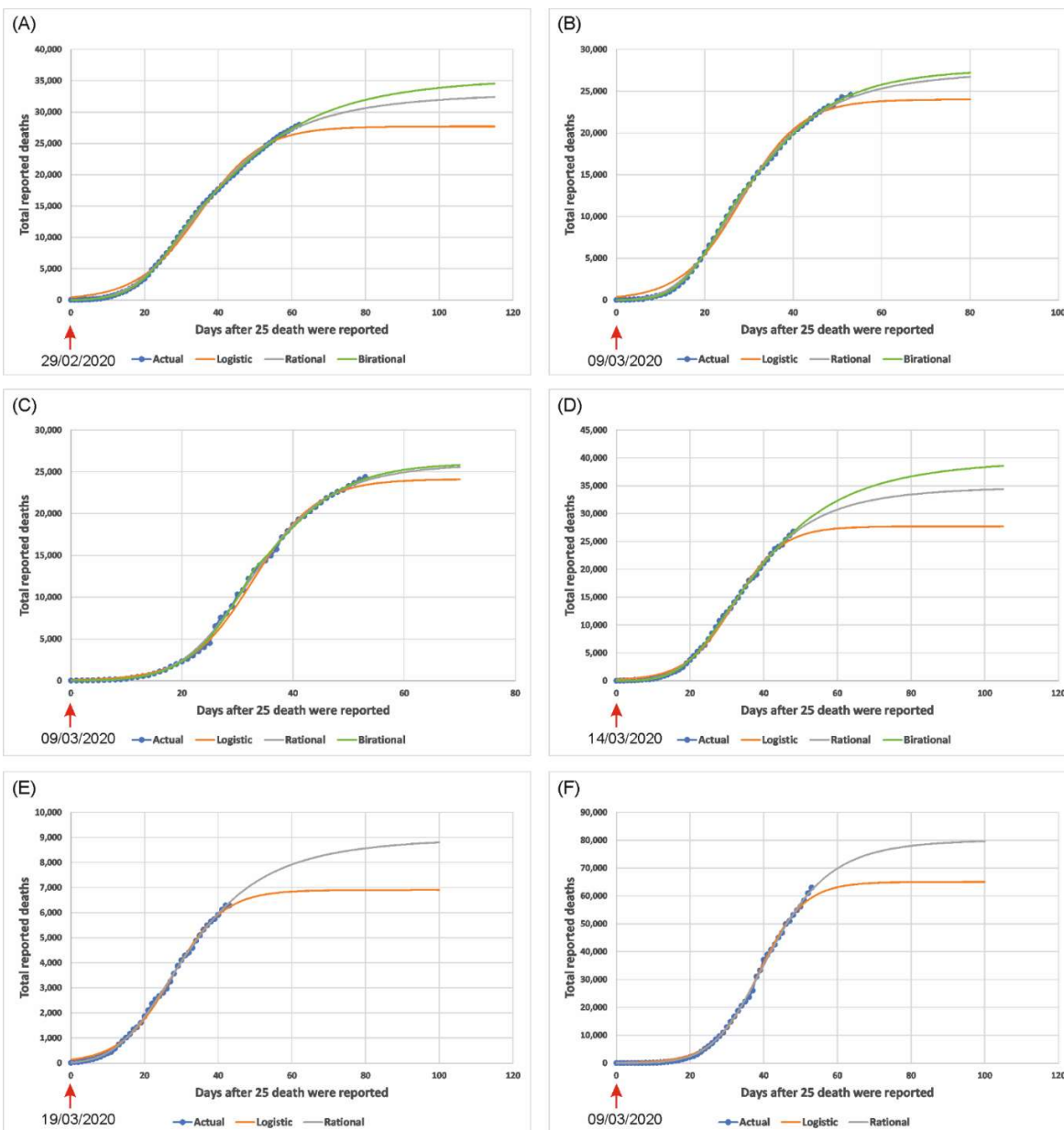
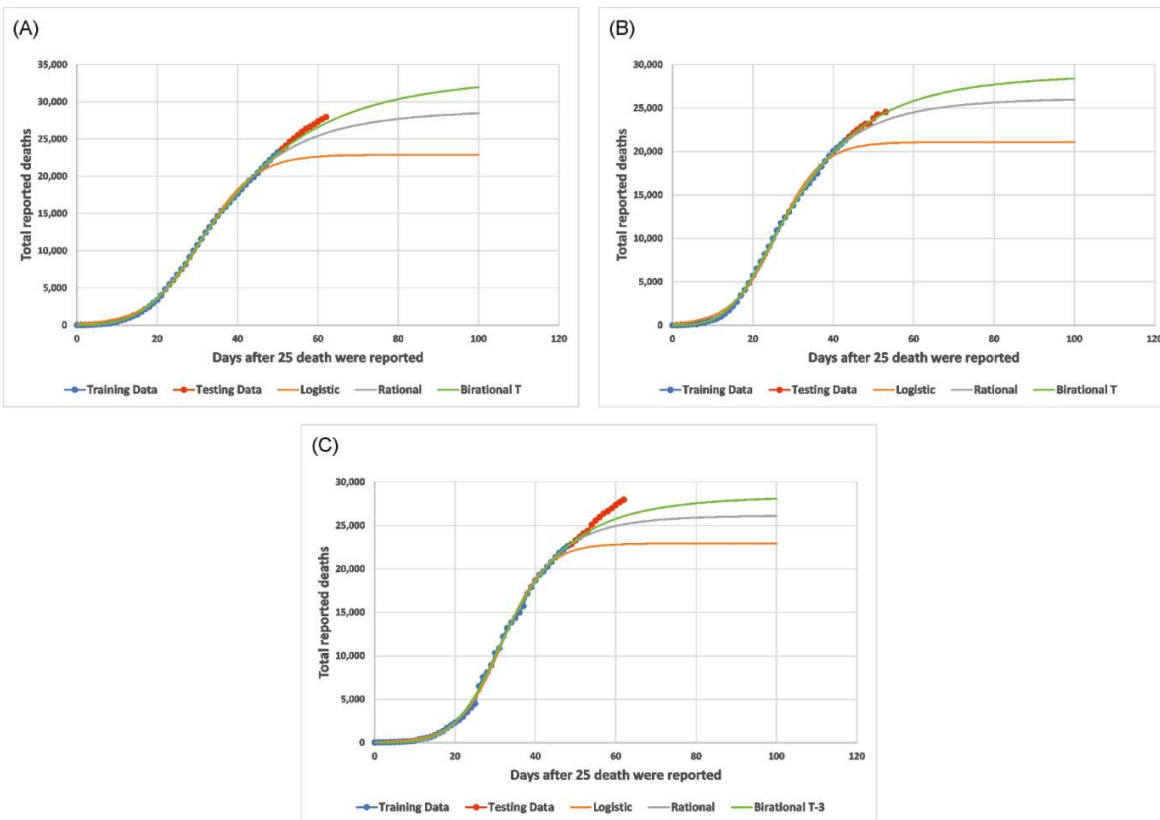


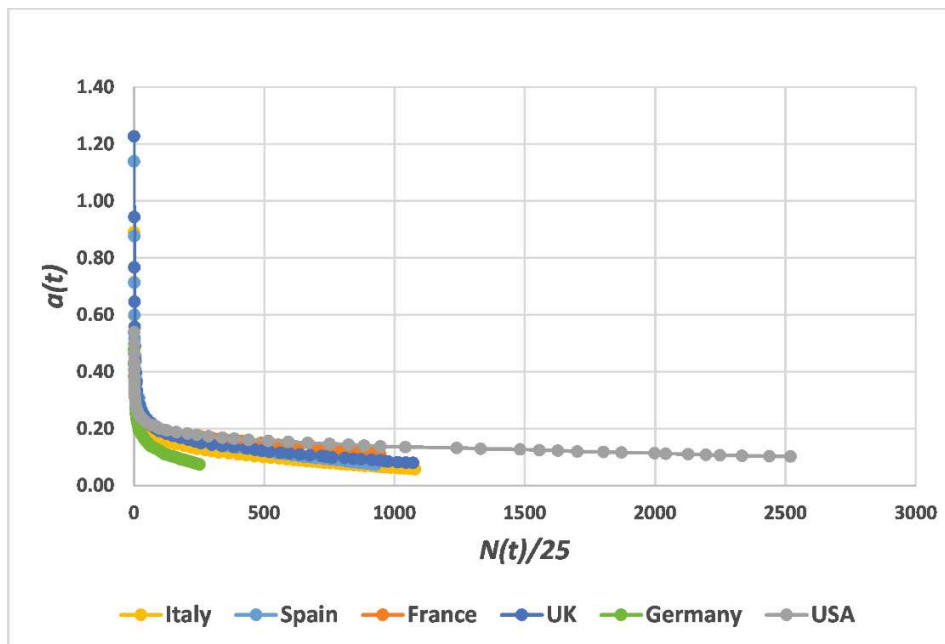
Fig. 2. Actual vs Predicted SARS-CoV-2 deaths for South Korea. The Actual vs the Predicted cumulative number of reported deaths, due to SARS-CoV-2, are presented in (A) as a function of days after 25 deaths were reported for South Korea. A closer view of the fitted data is presented in (B). The three models were trained using data up to May 1, 2020 ($t=60$). The inflection point occurred at $t=23$ which corresponds to March 25, 2020.



433 **Fig. 3. Actual vs Predicted SARS-CoV-2 deaths for various countries.** The Actual vs the
434 Predicted cumulative number of reported deaths, due to SARS-CoV-2, are presented as a function
435 of days after 25 deaths were reported, for: (A) Italy, (B) Spain, (C) France, (D) UK, (E) Germany,
436 (F) USA. The three models were trained with data up to May 1, 2020. This corresponds to $t=62$
437 data points for Italy, $t=53$ data points for Spain, $t=53$ data points for France, $t=48$ data points for
438 UK, $t=43$ data points for Germany, and $t=53$ data points for USA. The inflection point occurs on
439 April 4, 2020, for Italy; on April 6, 2020, for Spain; on April 11, 2020, for France; on April 15,
440 2020, for UK; on April 15, 2020, for Germany; and on April 17, 2020, for USA.
441



444
 445 **Fig. 4. Predictions using a smaller training data set.** Predictions using a smaller training data set
 446 for the cumulative number of reported deaths as a function of days after 25 deaths were reported
 447 for: (A) Italy, (B) Spain and (C) France. The prediction fits were obtained using training data up to
 448 T+15 for each country, which corresponds to $t=50$, $t=43$ and $t=48$, for Italy, Spain and France,
 449 respectively.



450
 451 **Fig. 5. Plot of $a(t)$ as a function of $N(t)/25$ for the COVID-19 virus infection.** The function $a(t)$
 452 is plotted as a function of $N(t)/25$ for Italy, Spain, France, UK, Germany, and USA. For these
 453 countries, after t around T-7, $a(t)$ becomes the same linear function of $N(t)$.